Pion form factor from all-to-all propagators of overlap quarks

JLQCD collaboration: T. Kaneko[*a,b†], **H. Fukaya**[c], **S. Hashimoto**[a,b], **H. Matsufuru**[a],
J. Noaki[a], **T. Onogi**[d] **and N. Yamada**[a,b]

[a] *High Energy Accelerator Research Organization (KEK), Ibaraki 305-0801, Japan*

[b] *School of High Energy Accelerator Science, The Graduate University for Advanced Studies
(Sokendai), Ibaraki 305-0801, Japan*

[c] *Theoretical Physics Laboratory, RIKEN, Saitama 351-0198, Japan*

[d] *Yukawa Institute for Theoretical Physics, Kyoto University, Kyoto 606-8502, Japan*

We report on our calculation of the pion electromagnetic form factor with two-flavors of dynamical overlap quarks. Gauge configurations are generated using the Iwasaki gauge action on a $16^3 \times 32$ lattice at the lattice spacing of 0.12 fm with sea quark masses down to $m_s/6$, where m_s is the physical strange quark mass. We describe our setup to measure the form factor through all-to-all quark propagators and present preliminary results.

The XXV International Symposium on Lattice Field Theory
July 30-4 August 2007
Regensburg, Germany

[*]Speaker.

[†]E-mail: takashi.kaneko@kek.jp

1. Introduction

Since the pion plays a central role in low-energy dynamics, its properties are of great interest. For the electromagnetic form factor $F_\pi(q^2)$, precise experimental data are available near the zero momentum transfer $q^2 = 0$, where the dependence of $F_\pi(q^2)$ on the quark mass m and q^2 can be described by chiral perturbation theory (ChPT) provided that m is sufficiently small. A detailed comparison of $F_\pi(q^2)$ on the lattice with ChPT and experiments therefore provides a good testing ground for lattice calculations in the chiral regime. An understanding on the applicability of ChPT to lattice data is also helpful towards a reliable calculation of form factors of K, D and B mesons.

In this article, we report on our on-going calculation of $F_\pi(q^2)$ in two-flavor QCD. We employ the overlap fermions, which have the exact chiral symmetry and hence allow us to apply ChPT straightforwardly to our chiral extrapolation. The salient feature of this study is that $F_\pi(q^2)$ is calculated precisely through all-to-all quark propagators [1] for a meaningful comparison with ChPT and experiments.

2. Simulation method

We simulate QCD with two flavors of degenerate up and down quarks using the Iwasaki gauge action and the overlap quark action with the standard Wilson Dirac kernel. To reduce the computational cost substantially, (near-)zero modes of the kernel are suppressed by introducing two-flavors of unphysical Wilson fermions and twisted mass ghosts [2], which do not change the continuum limit. Our numerical simulations are carried out on a $N_s^3 \times N_t = 16^3 \times 32$ lattice at a single value of $\beta = 2.30$. The lattice spacing is $a = 0.1184(16)$ fm, if $r_0 = 0.49$ fm is used as input. We take four quark masses $m = 0.015, 0.025, 0.035$ and 0.050, which cover a range of $[m_s/6, m_s/2]$. Our current statistics are 50 configurations separated by 100 HMC trajectories at each m. So far, we have simulated only the trivial topological sector, and effects of the fixed global topology by the extra Wilson fermions are to be studied [3]. We refer to Ref.[4] for further details on our production run.

3. Measurement through all-to-all propagators

We construct all-to-all propagators of overlap quarks along the strategy proposed in Ref. [1]. Low-lying modes of the overlap operator D are determined by the implicitly restarted Lanczos algorithm and their contribution to the all-to-all propagator is calculated exactly as

$$(D^{-1})_{\text{low}} = \sum_{k=1}^{N_{\text{ep}}} \frac{1}{\lambda^{(k)}} u^{(k)} u^{(k)\dagger}, \tag{3.1}$$

where $(\lambda^{(k)}, u^{(k)})$ represents k-th eigenmode and the number of eigenmodes N_{ep} is set to 100 in this study. We note that the overlap operator is normal and the left and right eigenvectors coincide with each other.

The contribution of higher modes is estimated stochastically by the noise method with the dilution technique [1]. One Z_2 noise vector is generated for each configuration, and is *diluted* into $N_d = 3 \times 4 \times N_t/2$ vectors with support on a single value for color and spinor indices and at two

time-slices. The high mode contribution

$$(D^{-1})_{\text{high}} = \sum_{d=1}^{N_d} x^{(d)} \eta^{(d)\dagger} \tag{3.2}$$

can be obtained by solving the linear equation for each diluted source

$$Dx^{(d)} = (1 - P_{\text{low}})\eta^{(d)} \; (d = 1,...,N_d), \tag{3.3}$$

where d is the index for the dilution and P_{low} is the projector to the eigenspace spanned by the low modes. We employ the four dimensional relaxed CG for our overlap solver [5].

In summary, all-to-all quark propagators can be expressed as the matrix

$$D^{-1} = \sum_{k=1}^{N_{\text{vec}}} v^{(k)} w^{(k)\dagger} \quad (N_{\text{vec}} = N_{\text{ep}} + N_d) \tag{3.4}$$

constructed from the following two set of vectors v and w:

$$v^{(k)} = \left\{ \frac{u^{(1)}}{\lambda^{(1)}}, \dots, \frac{u^{(N_{\text{ep}})}}{\lambda^{(N_{\text{ep}})}}, x^{(1)}, \dots, x^{(N_d)} \right\}, \quad w^{(k)} = \left\{ u^{(1)}, \dots, u^{(N_{\text{ep}})}, \eta^{(1)}, \dots, \eta^{(N_d)} \right\}. \tag{3.5}$$

Then, two-point functions with the source (sink) operator at time-slice $t^{(\prime)}$ and three-point functions with the vector current at t'' can be expressed as

$$C_{\Gamma\Gamma',\phi\phi'}(t'-t;\mathbf{p}) = \sum_{k,l=1}^{N_{\text{vec}}} \mathcal{O}_{\Gamma',\phi'}^{(k,l)}(t',\mathbf{p}) \, \mathcal{O}_{\Gamma,\phi}^{(l,k)}(t,-\mathbf{p}), \tag{3.6}$$

$$C_{\Gamma\gamma_\mu\Gamma',\phi\phi'}(t''-t,t'-t'';\mathbf{p},\mathbf{p}') = \sum_{k,l,m=1}^{N_{\text{vec}}} \mathcal{O}_{\Gamma',\phi'}^{(m,l)}(t',\mathbf{p}') \, \mathcal{O}_{\gamma_\mu,\phi_l}^{(l,k)}(t'',\mathbf{p}-\mathbf{p}') \, \mathcal{O}_{\Gamma,\phi}^{(k,m)}(t,-\mathbf{p}), \tag{3.7}$$

where the momentum and smearing function for the initial (final) meson are denoted by $\mathbf{p}^{(\prime)}$ and $\phi^{(\prime)}$, and

$$\mathcal{O}_{\Gamma,\phi}^{(k,l)}(t,\mathbf{p}) = \sum_{\mathbf{x},\mathbf{r}} \phi(\mathbf{r}) \, w(\mathbf{x}+\mathbf{r},t)^{(k)\dagger} \, \Gamma \, v(\mathbf{x},t)^{(l)} \, e^{-i\mathbf{px}} \tag{3.8}$$

is the meson operator with the Dirac spinor structure Γ constructed from the v and w vectors. The smearing function for the local operator is $\phi_l(\mathbf{r}) = \delta_{\mathbf{r},\mathbf{0}}$.

We prepare the v and w vectors on the IBM BlueGene/L at KEK. The computational cost of the determination of low modes is ~ 0.6 TFLOPS $\cdot$ hours per configuration. Solving Eq. (3.3) is the most time-consuming part in our measurement, since it requires $N_t/2$ times more inversions than the conventional method. We observe that, however, the low-mode preconditioning of our overlap solver leads to about a factor of 8 speedup and its cost is reduced to ~ 1.7 TFLOPS $\cdot$ hours/conf for a given valence quark mass m. The calculation of the meson operator $\mathcal{O}_{\Gamma,\phi}^{(k,l)}(t,\mathbf{p})$ needs much less CPU time than the above two steps: it is about 0.2 GFLOPS $\cdot$ hours/conf for a single choice of $(m,\mathbf{p},\Gamma,\phi)$. The calculation of correlation functions are even less costly. These calculations are carried out on the Hitachi SR11000 and workstations at KEK.

The key issue in the all-to-all calculation is the re-usability of the all-to-all propagators: namely, we do not have to repeat the time-consuming Lanczos step and overlap solver to construct the meson operator $\mathscr{O}_{\Gamma,\phi}^{(k,l)}(t,\mathbf{p})$ for different choices of $(\mathbf{p},\Gamma,\phi)$. This is a great advantage in studies of form factors, which require an accurate estimate of relevant correlation functions with various choices of the momentum configuration $(\mathbf{p},\mathbf{p}')$. In this study, we test two smearing functions $\phi_l(\mathbf{r})$ and $\phi_s(\mathbf{r})=\exp[-0.4|\mathbf{r}|]$, and take 33 choices for the meson momentum $\mathbf{p}$ with $|\mathbf{p}|\leq 2$. Note that the lattice momentum is in units of $2\pi/L$ in this article. This setup enables us to simulate 11 different values of q^2, which cover a range of -1.65 [GeV^2] $\lesssim q^2$.

Figure 1: Jackknife data of three-point function $C_{\gamma_5\gamma_4\gamma_5,\phi_s\phi_s}(N_t/4,N_t/4;\mathbf{p},\mathbf{0})$ with $|\mathbf{p}| = \sqrt{2}$ before (top panel) and after averaging over source operator locations and momentum configurations (bottom panel). Data are normalized by the statistical average.

It is also advantageous to average the correlation functions over the momentum configurations, which give the same value of q^2, as well as over the source locations $(\mathbf{x},t)$ with temporal separations, namely $\Delta t = t''-t$ and $\Delta t' = t'-t''$, kept fixed. This averaging reduces the statistical fluctuation remarkably as shown in Fig. 1.
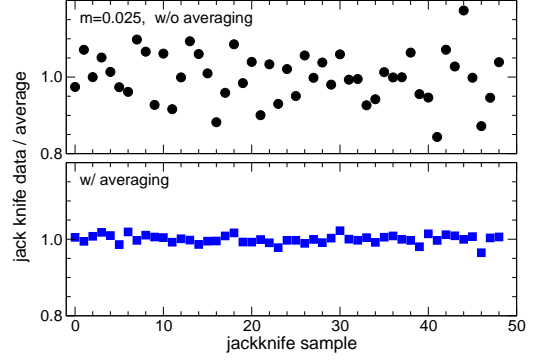
4. Pion form factor and charge radius

We calculate effective value of the pion form factor from the ratio

$$F_{\pi,\phi}(\Delta t,\Delta t';q^2) = \frac{2M_\pi}{E_\pi(|\mathbf{p}|)+E_\pi(|\mathbf{p}'|)}\frac{R_\phi(\Delta t,\Delta t';|\mathbf{p}|,|\mathbf{p}'|,q^2)}{R_\phi(\Delta t,\Delta t';0,0,0)}, \qquad (4.1)$$

$$R_\phi(\Delta t,\Delta t';|\mathbf{p}|,|\mathbf{p}'|,q^2) = \frac{C_{\gamma_5\gamma_4\gamma_5,\phi\phi}(\Delta t,\Delta t';\mathbf{p},\mathbf{p}')}{C_{\gamma_5\gamma_5,\phi\phi_l}(\Delta t;\mathbf{p})\,C_{\gamma_5\gamma_5,\phi_l\phi}(\Delta t';\mathbf{p}')}, \qquad (4.2)$$
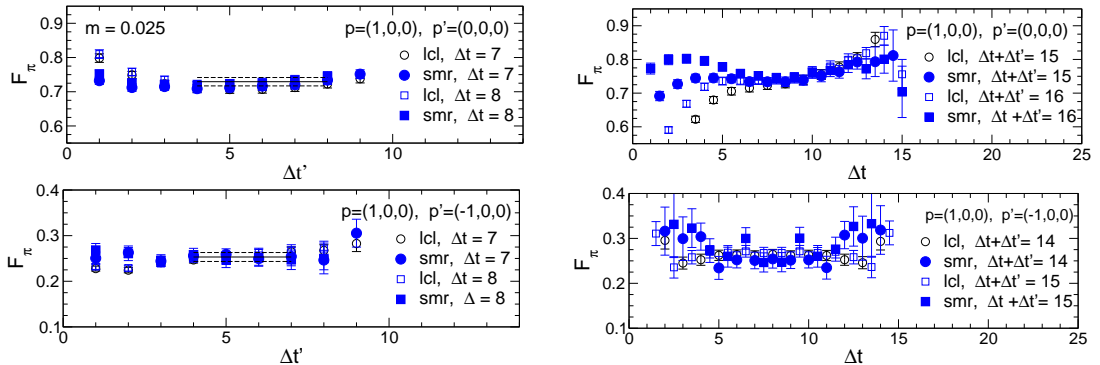

Figure 2: Effective value of pion form factor $F_{\pi,\phi}(\Delta t,\Delta t';q^2)$ at $m=0.025$. In the left panels, the data are plotted as a function of $\Delta t'$ with Δt fixed, whereas the right panels show Δt dependence with $\Delta t + \Delta t'$ fixed. Open (filled) symbols show data with $\phi = \phi_l$ (ϕ_s).
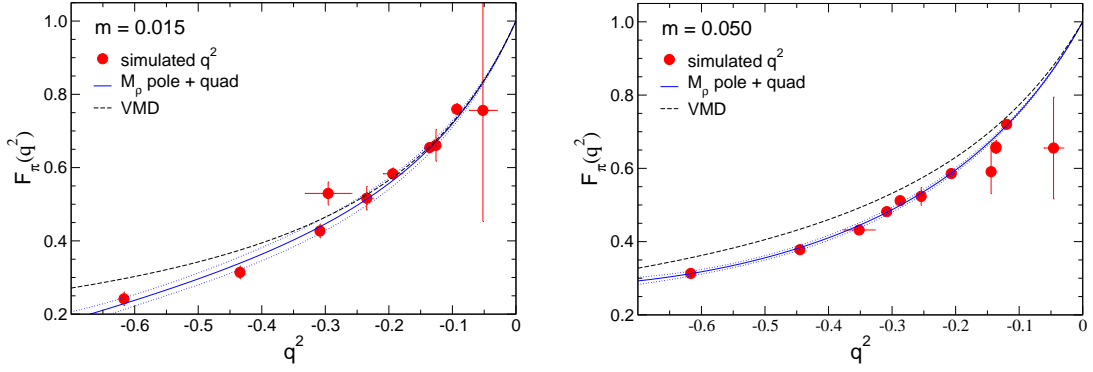
Figure 3: Pion form factor at $m = 0.015$ (left panel) and 0.050 (right panel) as a function of q^2. The Solid line shows the parametrization of the measured pole plus the quadratic correction. The dashed line is the expectation from VMD.

where $\phi = \phi_l$ or ϕ_s, and the pion mass M_π and energy E_π are determined by single-cosh fits to $C_{\gamma_5\gamma_5,\phi_s\phi_s}$. We note that the ratio R_ϕ is calculated from correlation functions averaged over the momentum configurations and source locations.

An example of $F_{\pi,\phi}(\Delta t, \Delta t'; q^2)$ is plotted in Fig. 2. The pion form factor $F_\pi(q^2)$ is determined from a constant fit to $F_{\pi,\phi_s}(\Delta t, \Delta t'; q^2)$ in a range of $(\Delta t, \Delta t')$, where F_{π,ϕ_s} shows a reasonable plateau and good agreement with data with $\phi = \phi_l$. As shown in Fig. 3, we obtain an accurate estimate of $F_\pi(q^2)$ except at our smallest q^2, where $C_{\gamma_5\gamma_4\gamma_5,\phi\phi}$ suffers from the most serious damping factor $e^{-E_\pi(|\mathbf{p}|)\Delta t}e^{-E_\pi(|\mathbf{p}'|)\Delta t'}$ with $(|\mathbf{p}|, |\mathbf{p}'|) = (2, 1)$.

In the same figure, we observe that the q^2 dependence of our data is close to the expectation from the vector meson dominance (VMD) hypothesis $F_\pi(q^2) \sim 1/(1 - q^2/M_\rho^2)$ particularly near $q^2 = 0$. The q^2 dependence is therefore parametrized by the following form of the vector meson pole with a polynomial (up to cubic order)

$$F_\pi(q^2) = \frac{1}{1 - q^2/M_\rho^2} + c_1 q^2 + c_2 q^4 + c_3 q^6, \tag{4.3}$$

or an additional pole correction

$$F_\pi(q^2) = \frac{c}{1 - q^2/M_\rho^2} + \frac{c'}{1 - q^2/M_{\text{pole}}^2} \quad (c + c' = 1). \tag{4.4}$$

While the simplest form Eq. (4.3) with the linear correction $(c_2, c_3 = 0)$ gives a slightly high value of $\chi^2/\text{dof} \gtrsim 2$ at heavier quark masses $m \geq 0.035$, other fitting forms describe our data reasonably well at all m.

In Fig. 4, we compare the charge radius

$$\langle r^2 \rangle = 6 dF_\pi(q^2)/dq^2 \big|_{q^2=0} \tag{4.5}$$

obtained from different fitting forms and range for the parametrization of the q^2 dependence. Our result is quite stable against variation of these fitting setup. In the following, we employ Eq. (4.3) with the quadratic correction, since it gives the least value of χ^2/dof with reasonably well-determined fitting parameters. We include the leading finite volume correction [6] into the result for $\langle r^2 \rangle$.

Figure 5 shows our chiral extrapolation of $\langle r^2 \rangle$. In this preliminary report, we test the NLO ChPT formula [7]

$$\langle r^2 \rangle = c_0 + \frac{1}{(4\pi f_0)^2} \log \left[M_\pi^2 \right] + c_1 M_\pi^2, \quad (4.6)$$

where a higher order analytic correction is included to account for the quark mass dependence of the contribution of the vector resonance $6/M_\rho^2$. With two values of f_0 from our studies in p- and ε-regimes [8], Eq. (4.6) gives a reasonable value of $\chi^2/\mathrm{dof} \sim 1.2$ even without the higher order term. It is however likely that this consistency with NLO ChPT is accidental, since, as seen Fig. 5, the quark mass dependence of our data is mainly caused by that of the resonance contribution.

Figure 4: Charge radius obtained at $m = 0.025$ from various choices of fitting form (left panel) and lower cut for fit range in parametrization of q^2 dependence of $F_\pi(q^2)$ (right panel).

This chiral extrapolation leads to our preliminary result

$$\langle r^2 \rangle = 0.388(9)_{\mathrm{stat}}(12)_{\mathrm{sys}} \, \mathrm{fm}^2, \quad (4.7)$$

where the systematic error is estimated by changing the parametrization form of the q^2 dependence of $F_\pi(q^2)$ and the choice of f_0, and by removing the higher order correction in Eq. (4.6). This result is significantly smaller than the experimental value $0.452(11)$ fm [9]. We need further investigations on systematic uncertainties: namely the lattice scale has to be fixed from an experimental input and we need study finite volume effects including those due to the fixed topology [3]. The consistency with ChPT may also be tested within the framework including resonance contributions [10] as in an analysis of experimental data in Ref [11].

5. Conclusions

In this article, we report on our calculation of $F_\pi(q^2)$ in two-flavor QCD through all-to-all
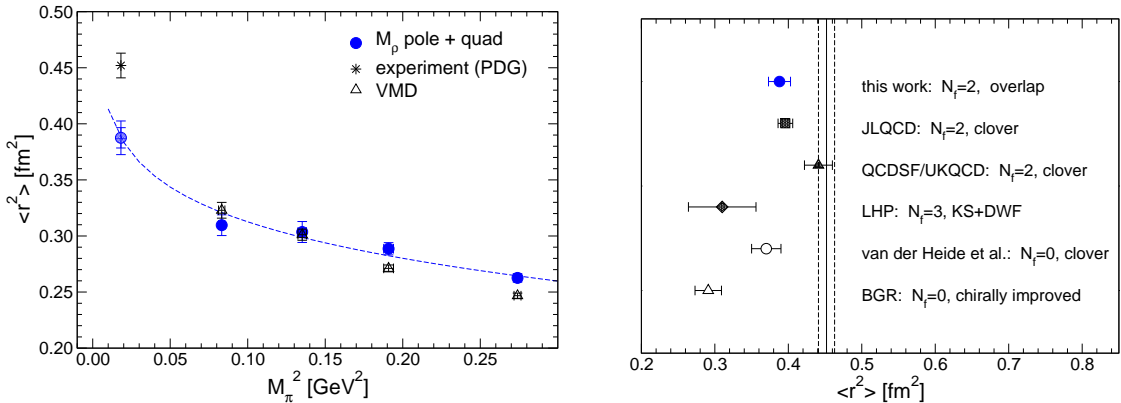

Figure 5: Left panel: chiral extrapolation of charge radius $\langle r^2 \rangle$. The experimental value in Ref.[9] and $\langle r^2 \rangle = 6/M_\rho^2$ from VMD are alto plotted. Right panel: comparison of $\langle r^2 \rangle$ from recent studies.
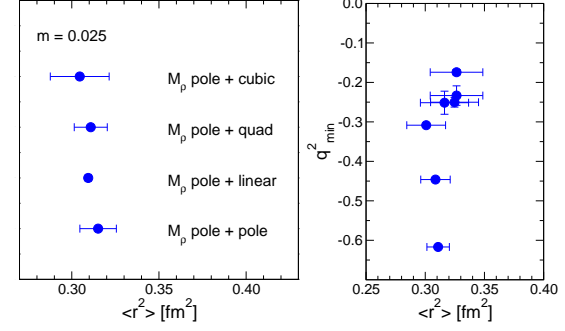
propagators of the overlap fermions. Our preliminary result for $\langle r^2 \rangle$ is a slightly smaller than experiment as in most of previous studies [12, 13, 14, 15, 16, 17] shown in Fig. 5. To understand the source of this discrepancy, we are completing our measurement of $F_\pi(q^2)$ with our full statistics (10,000 trajectories at each m) for a more stringent comparison with experiment and ChPT.

We also observe that the all-to-all propagators provide a very precise determination of meson correlators. Our studies are already underway for the pion scalar form factor, $K \to \pi$ form factors and flavor singlet mesons using meson operators Eq. (3.8) saved to disk.

References

[1] J. Foley *et al.* (TrinLat collaboration), Comput. Phys. Commun, **172**, 145 (2005) [arXiv:hep-lat/0505023].

[2] P.M. Vranas, arXiv:hep-lat/0001006; Phys. Rev. D **74**, 034512 (2006) [arXiv:hep-lat/0606014]; T. Izubuchi and C. Dawson (RBC collaboration), Nucl. Phys. B (Proc.Suppl.) **106**, 748 (2002); H. Fukaya *et al.* (JLQCD collaboration), Phys. Rev. D **74**, 094505 (2006) [hep-lat/0607020].

[3] R. Brower, S. Chandrasekharan, J.W. Negele and U.-J. Wiese, Phys. Lett. B **560**, 64 (2003) [arXiv:hep-lat/0302005]; S. Aoki, H. Fukaya, S. Hashimoto and T. Onogi, arXiv:0707.0396.

[4] H. Matsufuru, these proceedings.

[5] N. Cundy *et al.*, Comput. Phys. Commun. **165**, 221 (2005) [arXiv:hep-lat/0405003].

[6] B. Borasoy and R. Lewis, Phys. Rev. D **71**, 014033 (2005) [arXiv:hep-lat/0410042]; T.B. Bunton, F.-J. Jiang and B.C. Tiburzi, Phys. Rev. D **74**, 034514 (2006) [arXiv:hep-lat/0607001, Erratum-ibid. D **74**, 099902 (2006)].

[7] J. Gasser and H. Leutwyler, Ann. Phys. **158**, 142 (1984).

[8] J. Noaki (JLQCD collaboration), these proceedings; H. Fukaya (JLQCD collaboration), these proceedings.

[9] W.-M. Yao *et al.* (Particle Data Group), J. Phys. G **33**, 1 (2006).

[10] G. Ecker, J. Gasser, A.Pich and E. de Rafael, Nucl. Phys. B **321**, 311 (1989).

[11] J. Bijnens, G. Colangelo and P. Talavera, JHEP **9805**, 014 (1998) [arXiv:hep-ph/9805389].

[12] J. van der Heide, J.H. Koch and E. Laermann, Phys. Rev. D **69**, 094511 (2004) [arXiv:hep-lat/0312023].

[13] F.D.R. Bonnet *et al.* (LHP collaboration), Phys. Rev. D **72**, 054506 (2005) [arXiv:hep-lat/0411028].

[14] S. Hashimoto *et al.* (JLQCD collaboration), PoS **LAT2005**, 336 (2005) [arXiv:hep-lat/0510085].

[15] S. Capitani, C. Gattringer and C.B. Lang (BGR collaboration), Phys. Rev. D **73**, 034505 (2006) [arXiv:hep-lat/0511040].

[16] D. Brömmel *et al.* (QCDSF/UKQCD collaboration), arXiv:hep-lat/0608021.

[17] For a recent review, see Ph. Hägler, these proceedings.